

Gapless Edge-Modes and Topology in the Qi-Wu-Zhang Model A Real-Space Analysis

Arjo Dasgupta, Indra Dasgupta
*School of Physical Sciences,
Indian Association for the Cultivation of Science
2A & 2B, Raja Subodh Chandra Mallick Rd
Jadavpur, Kolkata, West Bengal 700032*

The topological phase transition in the Qi-Wu-Zhang model is studied, with particular attention to the appearance of chiral edge-modes in the nontrivial phase. Time-reversal symmetry breaking and its role in the topological phase transition is explicitly demonstrated. An effective Hamiltonian for the topologically protected edge-modes in a finite-size system is developed. The topological phase transition is understood in terms of a global perturbation to the system which lifts the degeneracy of the edge-modes.

I. INTRODUCTION

Chern insulators are two-dimensional materials which break time-reversal symmetry and are characterised by a *quantised Hall conductance* and the existence of *topologically protected chiral edge-modes*. Both these properties can be linked to a topological nontriviality, i.e., a *nonzero Chern number* [1],[2] calculated over the Brillouin Zone.

Several signatures characterising topologically nontrivial phases have been identified in the literature. The most well-known of these is the appearance of a Quantised Hall Conductance as in Haldane's original model for a Hall effect without Landau levels [3]. The obstruction to constructing localised degrees of freedom in nontrivial insulators has been recently exploited [4] to use the scaling properties of the localisation length to diagnose a topologically nontrivial phase.

Our aim in this paper is to *explain* the appearance of chiral edge-modes in the nontrivial phase of a 2D Chern insulator, namely the Qi-Wu-Zhang(QWZ) model [5], and develop a method for studying the topological phase transition in this model in terms of the edge-modes alone.

As discussed in [2], the topological phase transition in the QWZ model can be mapped to a corresponding topological phase transition in the Rice-Mele (RM) model for a 1D charge pump, making use of a technique known as *dimensional extension*. However, the dimensional extension technique rests on the bulk momentum-space Hamiltonian. This assumes periodic boundary conditions and thereby makes the physics at the edge of the system *inaccessible*.

In order to gain insight into the physical consequences of the topology of the system, we carry out a *real-space analysis* of the system with *open boundary conditions*. This gives us access to details about the difference in the structure of the wavefunctions

in the topologically trivial and nontrivial phases.

We identify a limit within the nontrivial phase of the QWZ model in which all eigenstates for a finite-size system can be determined in closed-form. We show that, through a variable transformation, this limit can be mapped to the familiar nontrivial flat-band limit of the Su-Schrieffer-Heeger Model [2],[6]. Considering the deviations from this exactly-solvable limit perturbatively, we construct an effective *edge-state Hamiltonian* which allows us to study the topological phase transition *in terms of the edge-modes alone*. We note that the two edge-modes are gapless throughout the nontrivial phase and that opening the gap requires a perturbation which changes the *global structure* of the system. We also find that the topological protection of the edge-modes depends on the *length* of the system, and becomes very weak for small system-sizes.

Our analysis of the QWZ model thus brings to light the significance of the Chern number *without any reference to the Brillouin Zone*, and thus may be extended to systems without lattice translation symmetry.

This paper is organised as follows. The bulk properties of the QWZ model are reviewed in section II. The role of time-reversal symmetry in the onset of the topological phase transition is discussed in section III. The properties of the nontrivial localised limit are illustrated in section IV and this limit is compared to the trivial atomic limit. Finally we illustrate a characterisation of the topological phase transition in terms of the edge-mode degeneracy in section V, followed by conclusions in section VI.

II. BULK PROPERTIES: A BRIEF REVIEW

The Qi-Wu-Zhang(QWZ) [5] model for a Chern insulator is the simplest possible model for a topological insulator defined on a square lattice. In order

to study the bulk properties of the model, it may be written in momentum space as:

$$H_{QWZ}(\mathbf{k}) = \lambda \sin(k_x a) \sigma_x + \lambda \sin(k_y a) \sigma_y + (1 + \lambda \cos(k_x a) + \lambda \cos(k_y a)) \sigma_z \quad (1)$$

This Hamiltonian may be constructed from the one-dimensional Rice-Mele model for adiabatic charge pumping as discussed in [2].

The dispersion-relation can be read off from 1 as:

$$E_{\pm}(\mathbf{k}) = \pm[\lambda^2 \sin^2(k_x a) + \lambda^2 \sin^2(k_y a) + (1 + \lambda \cos(k_x a) + \lambda \cos(k_y a))^2]^{\frac{1}{2}} \quad (2)$$

The spectrum is generally gapped. However the gap closes at two specific values of the parameter λ :

1. $\lambda = \frac{1}{2}$: the gap closes at $(k_x, k_y) = (\pm\frac{\pi}{a}, \pm\frac{\pi}{a})$.
2. $\lambda = -\frac{1}{2}$: the gap closes at $(k_x, k_y) = (0, 0)$.

shown in Fig. 1(a) and 1(b) respectively. Near these points, the dispersion relation is approximately linear: they are called *Dirac points*.

By decomposing $H(\mathbf{k})$ in terms of the Pauli matrices $(\sigma_x, \sigma_y, \sigma_z)$ as $\mathbf{d}(\mathbf{k}) \cdot \vec{\sigma}$ we find that the parameters trace out a torus in the three-dimensional parameter space given by:

$$\begin{aligned} d_x(\mathbf{k}) &= \lambda \sin(k_x a) \\ d_y(\mathbf{k}) &= \lambda \sin(k_y a) \\ d_z(\mathbf{k}) &= 1 + \lambda \cos(k_x a) + \lambda \cos(k_y a) \end{aligned}$$

The topology of the system is quantified by the Chern number n which tells us whether the torus encloses the point of degeneracy at the origin.

For $|\lambda| < \frac{1}{2}$ the torus entirely misses the origin and the system is topologically trivial (Chern number $n = 0$).

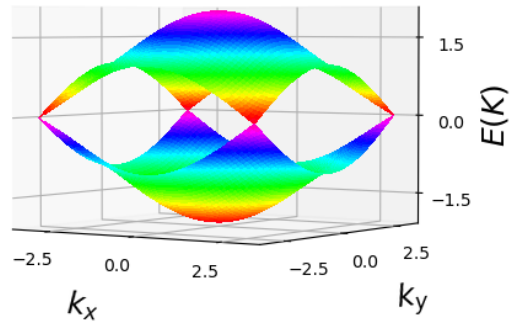
For $|\lambda| > \frac{1}{2}$, we have a nonzero Chern Number:

1. For $\lambda > \frac{1}{2}$, $n = 1$: the lower part of the torus encloses the origin (see Fig. 2(a)).
2. For $\lambda < -\frac{1}{2}$, $n = -1$: the orientation of the torus is reversed (see Fig. 2(b)).

The Chern number is a topological invariant which captures information about the *global structure* of the model as we shall see in section IV. Besides, the Kubo formula relates the Hall conductance of the system to the Chern number as: $\sigma_{xy} = \frac{e^2}{2\pi\hbar} n$. A detailed discussion of this *topological quantisation* of the Hall conductance may be found in [7].

Thus a topological phase transition takes place between $n = 0$ and $n = 1$ at $\lambda_c^+ = \frac{1}{2}$, and another between $n = 0$ and $n = -1$ at $\lambda_c^- = -\frac{1}{2}$.

(a) $\lambda = 0.5$



(b) $\lambda = -0.5$

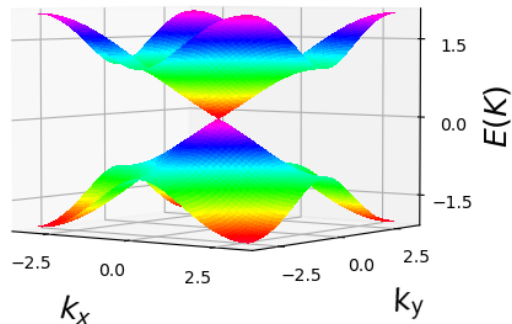


Figure 1: Gapless dispersion relations for the QWZ model: Dirac cones appear at (a) $(k_x, k_y) = (\pm\frac{\pi}{a}, \pm\frac{\pi}{a})$ for $\lambda = 0.5$ and (b) $(k_x, k_y) = (0, 0)$ for $\lambda = -0.5$

III. TIME-REVERSAL SYMMETRY BREAKING AND BAND INVERSION

From the discussion in the previous section we have established that the QWZ model shows a topological phase transition between the trivial phase with Chern number $n = 0$ and the nontrivial phase with $n = 1$ on crossing the parameter value $\lambda = \frac{1}{2}$. However, the analysis so far does not provide any physical justification for this topological phase transition.

In this section, we examine the role of *time-reversal symmetry-breaking* in Chern insulators and use this notion to study the topological phase transition in the QWZ model.

The Chern number on the 2D Brillouin Zone can be written as:

$$n = \frac{1}{4\pi} \int_{BZ} dS F(\mathbf{k})$$

Where $F(\mathbf{k})$ is the *Berry curvature* given by:

$$F(\mathbf{k}) = i \langle \nabla_{\mathbf{k}} u_{\mathbf{k}} | \times | \nabla_{\mathbf{k}} u_{\mathbf{k}} \rangle \quad (3)$$

with $\partial_{\alpha} = \frac{\partial}{\partial k_{\alpha}}$ and $|u_{\mathbf{k}}\rangle$ are the cell-periodic eigenstates of $H_{\mathbf{k}}$.

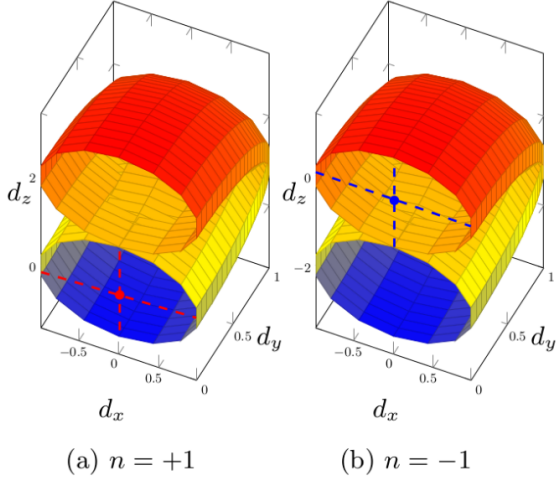


Figure 2: Systems with $\lambda > \frac{1}{2}$ and $\lambda < -\frac{1}{2}$ have opposite topologies: For $\lambda > \frac{1}{2}$ (a) the Chern number n is +1, while for $\lambda < -\frac{1}{2}$ (b), the orientation is reversed and $n = -1$

Under time-reversal $F(\mathbf{k})$ goes to $-F(-\mathbf{k})$, (see [1] for a detailed argument). Thus for a system with time-reversal symmetry $F(\mathbf{k}) = -F(-\mathbf{k})$, ensuring that the Chern number associated with such a system vanishes: $n = 0$.

Thus, in order to have a topologically nontrivial phase, it is *necessary* to break time-reversal symmetry.

In order to examine the role of time-reversal symmetry breaking in the QWZ model, we need to go over to a *real-space description* of the model. The momentum-space QWZ Hamiltonian may be written in the (a, b) sublattice basis as:

$$\begin{aligned}
 H(\mathbf{k}) &= \lambda e^{-ik_x a} \frac{\sigma_z + i\sigma_x}{2} + hc \\
 &+ \lambda e^{-ik_y a} \frac{\sigma_z + i\sigma_y}{2} + hc \\
 &+ \sigma_z
 \end{aligned} \quad (4)$$

This allows us to come up with a *real-space description* of the QWZ model: The model arises from the tight-binding approximation for hopping on a square lattice, with two orbitals a and b per lattice site. The real-space Hamiltonian may be written as:

$$H_{QWZ} = H_0 + \lambda H_1 + \lambda H_2 \quad (5)$$

Here H_0 is an onsite potential:

$$H_0 = \sum_{i=1}^N \sum_{j=1}^N \left(a_{i,j}^\dagger a_{i,j} - b_{i,j}^\dagger b_{i,j} \right)$$

H_1 is a standard nearest-neighbour hopping term involving the same orbital on neighbouring sites:

$$\begin{aligned}
 H_1 &= \frac{1}{2} \sum_{i=1}^{N-1} \sum_{j=1}^N \left(a_{i+1,j}^\dagger a_{i,j} - b_{i+1,j}^\dagger b_{i,j} + hc \right) \\
 &+ \frac{1}{2} \sum_{i=1}^N \sum_{j=1}^{N-1} \left(a_{i,j+1}^\dagger a_{i,j} - b_{i,j+1}^\dagger b_{i,j} + hc \right)
 \end{aligned}$$

Finally H_2 is a term mixing a and b orbitals on nearest-neighbours:

$$\begin{aligned}
 H_2 &= \frac{1}{2} \sum_{i=1}^{N-1} \sum_{j=1}^N \left(i a_{i+1,j}^\dagger b_{i,j} + i b_{i+1,j}^\dagger a_{i,j} + hc \right) \\
 &+ \frac{1}{2} \sum_{i=1}^N \sum_{j=1}^{N-1} \left(a_{i,j+1}^\dagger b_{i,j} - b_{i,j+1}^\dagger a_{i,j} + hc \right)
 \end{aligned}$$

Note that H_2 is asymmetric in the x and y directions. More importantly for us, the hopping along the x direction has a complex amplitude, *explicitly* breaking time-reversal symmetry.

In this model, $\lambda = 0$ describes the *flat-band* limit ($H = H_0$) of the QWZ model (see Fig. 3(a)). Time-reversal symmetry is preserved, and the Chern number thus vanishes: $n = 0$.

On tuning λ adiabatically between 0 and $\frac{1}{2}$, the bands acquire a dispersion (see Fig. 3(b)). The Chern number is only allowed to take integer values and thus cannot change abruptly on an adiabatic evolution of the parameters. The system thus remains in the trivial phase - breaking time-reversal symmetry alone is *not sufficient* to obtain a topologically nontrivial phase.

At $\lambda = \frac{1}{2}$, the gap in the bulk-dispersion closes at $(k_x, k_y) = (\pm \frac{\pi}{a}, \pm \frac{\pi}{a})$ (see Fig. 3(c)). Thus any deformation joining the $\lambda < \frac{1}{2}$ phase to the $\lambda > \frac{1}{2}$ phase violates adiabaticity, and leads to a change in the Chern number.

For parameter values $\lambda > \frac{1}{2}$, the system enters a nontrivial topological phase, with a sudden change in Chern number from $n = 0$ to $n = +1$ (see Fig. 3(d)), leading to the appearance of chiral edge-modes and a jump in the Hall conductance. This phase *cannot be adiabatically connected* to the trivial phase with $\lambda < \frac{1}{2}$.

The transition from the trivial phase to the nontrivial phase on passing through a bulk gap-closure at $\lambda_c = \frac{1}{2}$ is called *band inversion*.

The topology of the system is thus determined by a *competition* between the onsite term H_0 and the hopping term H_2 which breaks time-reversal symmetry. Note that the dispersion relations at $\lambda = 0.4$ and $\lambda = 0.6$ appear identical. The difference between the

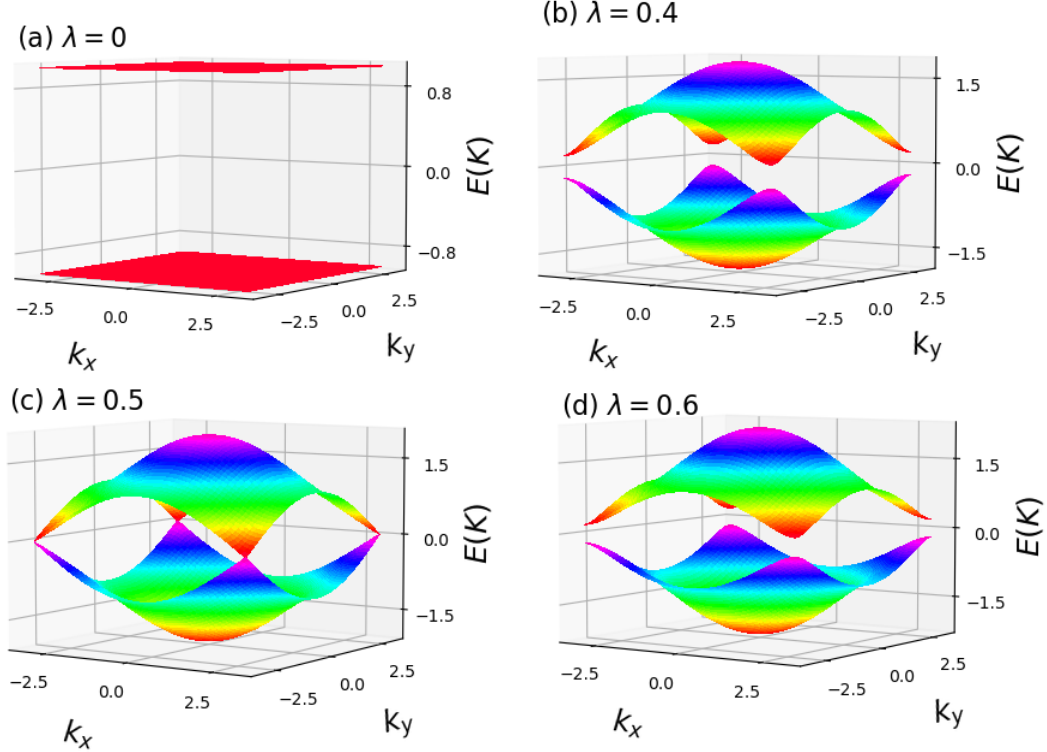


Figure 3: Topological phase transition in the QWZ model: for $\lambda = 0$ (a), the system has flat-bands. As λ is increased the bands acquire a dispersion. For $\lambda < \frac{1}{2}$ (b) the system has a trivial gap. The system becomes metallic at $\lambda = \frac{1}{2}$ (c) and for $\lambda > \frac{1}{2}$ (d) the gap becomes nontrivial. Note that the bulk-dispersion does in (b) and (d) are identical.

two phases is not apparent in the bulk physics but in the *topological effects which appear at the edge* which we shall explore further in the following section.

IV. DIMENSIONAL REDUCTION AND EXACTLY LOCALISED EDGE-MODES

In order to study the formation of edge-modes, we apply periodic boundary conditions in the y -direction and open boundary conditions in the x -direction. This allows us to take a Fourier transform along the y -direction and separate the full Hamiltonian H_{QWZ} into Hamiltonians describing one-dimensional lattices, each for a different value of k_y . This decomposition into one-dimensional chains is called *dimensional reduction* [9].

$$H_{QWZ} = \sum_{k_y} H_{1D}(k_y) \quad (6)$$

H_{1D} is defined on a 1D chain with an internal degree of freedom (a/b orbital) associated with each lattice site.

$$H_{1D} = \lambda(H_0 + H_1 + V) \quad (7)$$

Here H_0 is a hopping term which breaks time-reversal symmetry:

$$H_0 = \sum_{i=1}^{N-1} \frac{1}{2} [(a_{i+1}^\dagger a_i - b_{i+1}^\dagger b_i + hc) + (i a_{i+1}^\dagger b_i + i b_{i+1}^\dagger a_i + hc)]$$

H_1 mixes a and b orbitals at the same lattice site:

$$H_1 = \sum_{i=1}^N i \sin(k_y a) (b_i^\dagger a_i - a_i^\dagger b_i)$$

While V is an onsite term given by:

$$V = \sum_{i=1}^N \left(\frac{1}{\lambda} + \cos(k_y a) \right) (a_i^\dagger a_i - b_i^\dagger b_i)$$

Note that the operators of the form a_i^\dagger contain a k_y dependence which we have suppressed. a_{i,k_y}^\dagger acting

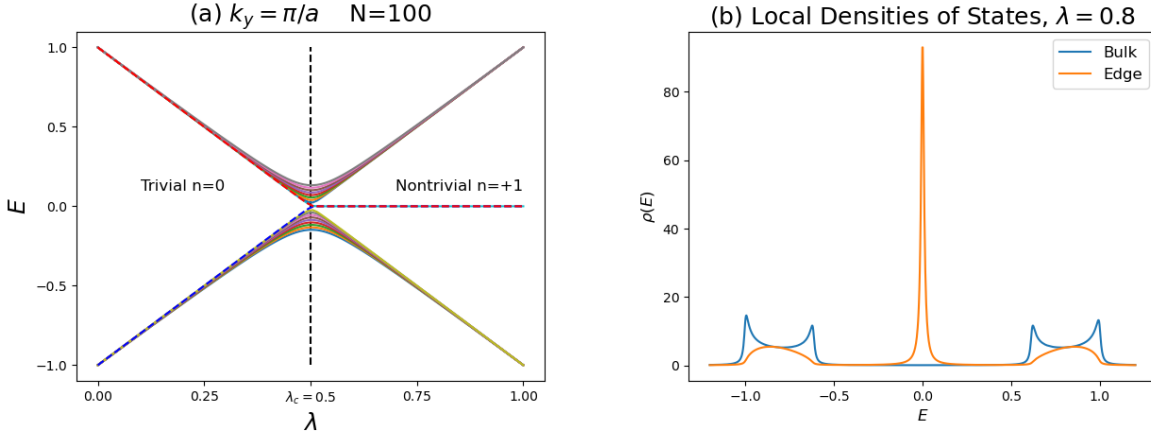


Figure 4: (a) Low energy levels for $H_{1D}(k_y = \frac{\pi}{a})$ on a lattice of 100 sites: zero-energy edge modes (shown as dashed lines) appear for $\lambda > \frac{1}{2}$. (b) Edge-modes lead to a peak at $E = 0$ in the local density of states at the edge.

on the vacuum state creates a mode with wavenumber k_y propagating along the y -direction localised on the orbital a at the site i on the x -axis.

As the Hamiltonian H_{QWZ} is quadratic, modes with different values of k_y are independent of each other, leaving us with a family of *decoupled* one-dimensional chains parameterised by k_y .

By placing the one-dimensional Hamiltonian H_{1D} on a finite lattice (100 sites), we have solved the eigenvalue problem numerically, and demonstrated the formation of edge modes for $\lambda > \lambda_c$ (see Fig. 4). As predicted, the edge-modes appear as λ crosses the critical value $\lambda_c = \frac{1}{2}$ (see Fig. 4(a)). As λ is increased further and the bulk gap opens, the edge-modes remain gapless.

The difference between the properties of the bulk and edge-states is captured by the local density of states:

$$\rho_i(E) = \sum_n |\langle i|n\rangle|^2 \delta(E - E_n) \quad (8)$$

Where the index n labels the energy-levels and i labels the lattice-sites.

For $\lambda > \frac{1}{2}$, the localised edge-modes give rise to a peak at $E = 0$ in the local density of states at the edges. No such peak appears in the bulk (see Fig. 4(b)).

To study the formation of low-energy edge-modes we look near the Dirac point by setting $k_y = \frac{\pi}{a} + q_y$ for $q_y \ll \frac{\pi}{a}$, with the system placed in the nontrivial phase ($\lambda > \frac{1}{2}$).

On choosing $\lambda = 1$ and considering only terms to first order in $q_y a$ allows the onsite term V drops out. At this order, the prefactor in H_1 is given by $-iq_y a$. Consider the state $|R\rangle = \frac{1}{\sqrt{2}}(|a_N\rangle - i|b_N\rangle)$ localised at the right edge of the system. This state is created

by the action of the operator $\Psi_R^\dagger = a_N^\dagger - ib_N^\dagger$ on the vacuum state. We find that Ψ_R^\dagger commutes with H_0 :

$$\begin{aligned} [H_0, \Psi_R^\dagger] &= [a_{N-1}^\dagger a_N, a_N^\dagger] + i[b_{N-1}^\dagger b_N, b_N^\dagger] \\ &\quad - i[b_{N-1}^\dagger a_N, a_N^\dagger] - [a_{N-1}^\dagger b_N, b_N^\dagger] \\ &= (a_{N-1}^\dagger - ib_{N-1}^\dagger)(b_N^\dagger b_N - a_N^\dagger a_N) \\ &\quad + (a_{N-1}^\dagger - ib_{N-1}^\dagger)(a_N^\dagger a_N - b_N^\dagger b_N) = 0 \end{aligned}$$

$|R\rangle$ is thus a zero-energy eigenstate of H_0 . $|R\rangle$ is also an eigenstate of H_1 :

$$H_1 |R\rangle = q_y a |R\rangle$$

We thus have $H_{1D} |R\rangle = q_y a |R\rangle$. Similarly, we have the eigenstate $|L\rangle = \frac{1}{\sqrt{2}}(|a_1\rangle + i|b_1\rangle)$ localised at the left edge of the system: $H_{1D} |L\rangle = -q_y a |L\rangle$.

On considering the group velocity $v_y = \frac{\partial E}{\partial q_y}$, we find that the left and right edge-modes conduct in opposite directions. They are thus called *chiral edge-modes*.

Motivated by the structure of these edge-modes, we define the new variables $|\psi_i\rangle = \frac{1}{\sqrt{2}}(|a_i\rangle - i|b_i\rangle)$ and $|\bar{\psi}_i\rangle = \frac{1}{\sqrt{2}}(|a_i\rangle + i|b_i\rangle)$.

Under the action of H_0 , the states $|\psi_i\rangle$ and $|\bar{\psi}_i\rangle$ transform as:

$$\begin{aligned} H_0 |\psi_i\rangle &= |\bar{\psi}_{i+1}\rangle \\ H_0 |\bar{\psi}_i\rangle &= |\psi_{i-1}\rangle \end{aligned} \quad (9)$$

The states $|\psi_i\rangle$ move to the right under the action of H_0 , while the states $|\bar{\psi}_i\rangle$ move to the left.

The states $|R\rangle = |\psi_N\rangle$ and $|L\rangle = |\bar{\psi}_1\rangle$ at the two edges of the chain thus have nowhere to go and are

annihilated by H_0 , i.e., they are zero-energy edge-modes of H_0 . The presence of the edge-modes make the system *gapless* even as the bulk of the system is insulating.

What happens in the bulk? Here too the states are localised: $|\psi_i\rangle$ and $|\bar{\psi}_{i+1}\rangle$ combine to form $2N - 2$ dimerised eigenstates (see Fig. 5(a)), $|\alpha_i\rangle = \frac{1}{\sqrt{2}}(|\psi_i\rangle + |\bar{\psi}_{i+1}\rangle)$ and $|\beta_i\rangle = \frac{1}{\sqrt{2}}(|\psi_i\rangle - |\bar{\psi}_{i+1}\rangle)$:

$$\begin{aligned} H_0 |\alpha_i\rangle &= |\alpha_i\rangle \\ H_0 |\beta_i\rangle &= -|\beta_i\rangle \end{aligned} \quad (10)$$

Written in terms of the variables $\psi_i, \bar{\psi}_i$, the Hamiltonian H_0 appear as:

$$H_0 = \sum_{i=1}^{N-1} (\Psi_i^\dagger \bar{\Psi}_{i+1} + hc) \quad (11)$$

In these new variables H_0 is identical to the nontrivial flat-band limit of the Su-Schrieffer-Heeger (SSH) model for topologically protected edge-states in polyacetylene introduced in [6]. For a more detailed discussion of the SSH model we refer the reader to Chapter 1 of [2].

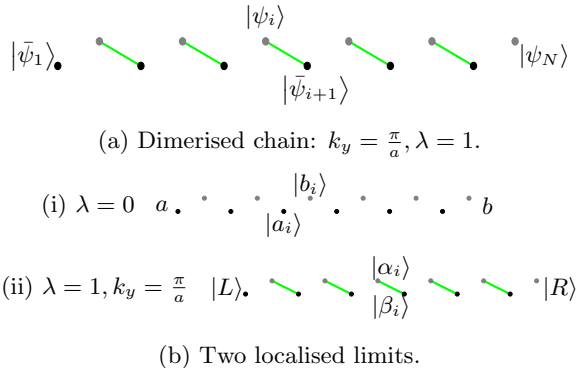


Figure 5: (a) The states ψ_i and $\bar{\psi}_{i+1}$ combine to form dimers, leaving two free ends. (b) The system hosts localised eigenstates at two limits: (i) The atomic limit at $\lambda = 0$, and (ii) $\lambda = 1, k_y = \frac{\pi}{a}$.

Note that the nearest-neighbour hopping always changes the sublattice. There are thus no diagonal terms in the sublattice basis. H_0 thus has chiral symmetry[8]: $\{H_0, \sigma_z\} = 0$.

In terms of the projectors onto the ψ and $\bar{\psi}$ sublattices, σ_z is given by:

$$\sigma_z = P_\psi - P_{\bar{\psi}}$$

As discussed in [5], chiral symmetry ensures that the eigenstates come in pairs called *chiral partners*,

$\{|n\rangle, \sigma_z |n\rangle\}$ such that if $H_0 |n\rangle = E_n |n\rangle$, then $H_0 \sigma_z |n\rangle = -E_n \sigma_z |n\rangle$.

Zero-energy states for models with chiral symmetry may be *restricted* to a single sublattice: for instance, $H_0 P_\psi |E_n = 0\rangle = \frac{1}{2} H_0 (1 - \sigma_z) |E_n = 0\rangle = 0$.

Chiral symmetry plays a crucial role in the localisation of the zero-energy edge-states. We have established that any zero-energy state must be restricted to either the ψ or the $\bar{\psi}$ sublattice. Now, all the states $|\psi_i\rangle$ are connected to the states $|\bar{\psi}_{i+1}\rangle$ by the action of H_0 , with the exception of $|\psi_N\rangle$ on the right edge. Thus any zero-energy eigenstate of H_0 on the ψ -sublattice must reside on the lattice site at the right edge of the system. A similar argument may be made for the left edge-state on the $\bar{\psi}$ -sublattice. Notably, the bands in the ($\lambda = 1, k_y = \frac{\pi}{a}$) limit are *flat*, just as in the case of the atomic limit $\lambda = 0$. In the latter case the states are restricted to individual atoms a_i and b_i . This localisation is controlled by time-reversal symmetry, and the system is topologically trivial.

On the other hand, dimerised flat-band limit ($\lambda = 1, k_y = \frac{\pi}{a}$) is topologically nontrivial. Despite breaking time-reversal symmetry, the states are localised as a consequence of the dimerisation which is allowed by the chiral symmetry of the chain (see Fig. 5(b)).

V. GAPLESSNESS AND THE TOPOLOGICAL PHASE TRANSITION

We have seen that the two phases of the QWZ model have two particularly simple flat-band limits, the atomic limit $\lambda = 0$ in the trivial phase and the dimerised flat-band limit ($\lambda = 1, k_y = \frac{\pi}{a}$) in the nontrivial phase. In the latter, we find two zero-energy edge-states restricted to the lattice sites at the two edges of the system.

In this section, we carry out a perturbative analysis within the subspace of the two edge-states on deviating from the $\lambda = 1$ limit, while keeping k_y fixed at $\frac{\pi}{a}$ to ensure that we encounter the Dirac point at $\lambda = \frac{1}{2}$. As we decrease λ from $\lambda = 1$ towards the critical point at $\lambda = \frac{1}{2}$, the onsite term V comes into play.

The states $|\psi_i\rangle$ and $|\bar{\psi}_i\rangle$ are connected by the action of V : $V |\psi_i\rangle = \xi |\bar{\psi}_i\rangle$ with $\xi = \frac{1}{\lambda} - 1$. In effect, V acts as a *hopping term* for the localised states and thus leads to the delocalisation of both the bulk and the edge-states (see Fig. 6(a)).

In order for the edge-state $|R\rangle$ to mix with the other edge-state $|L\rangle$, it has to hop across the entire length of the chain. For a lattice of N sites, the degeneracy of the two states is broken by V through a process of order N . Below this order, the edge-modes remain gapless.

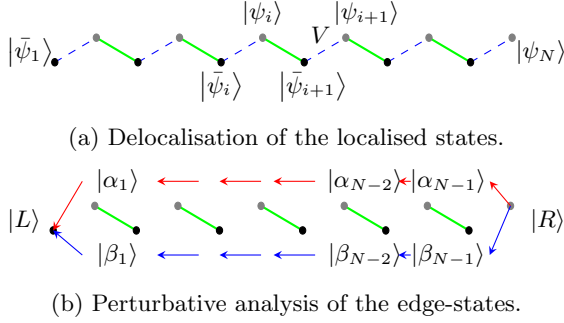


Figure 6: (a) The localised eigenstates of H_0 delocalise under the action of the onsite term V . (b) Intermediate states for shortest path between $|R\rangle$ and $|L\rangle$. Hopping from the states $|\alpha\rangle$ to the states $|\beta\rangle$ is not allowed, drastically reducing the number of possible paths.

In order to study the effect of V at this order we make use of Brillouin-Wigner perturbation theory, as discussed in [10], to construct an *effective Hamiltonian* in the edge-state subspace, taking into account the effects of mixing with the bulk-states. An eigenstate $|n\rangle$ of the unperturbed Hamiltonian H_0 , receives a correction $|n^{(m)}\rangle$ at order m given by:

$$|n^{(m)}\rangle = \sum_{\zeta_m, \dots, \zeta_1} |\zeta_m\rangle \frac{1}{E_n - \epsilon_{\zeta_m}} \langle \zeta_m | V | \zeta_{m-1} \rangle \times \dots \times |\zeta_1\rangle \frac{1}{E_n - \epsilon_{\zeta_1}} \langle \zeta_1 | V | n \rangle$$

Here E_n denotes the energy corresponding to the eigenstate $|N\rangle$ of the full Hamiltonian $H_0 + V$. The sum is carried out over the intermediate states $\{|\zeta_m\rangle\}$ which are nondegenerate with the unperturbed state $|n\rangle$.

In our case, we start out from the unperturbed eigenstate $|R\rangle$ of the system. To reach the other end $|L\rangle$ of the chain in N steps, there are 2 possible sets of intermediate states: $\{\alpha_{N-1}, \dots, \alpha_1\}$ or $\{\beta_{N-1}, \dots, \beta_1\}$ (see Fig. 6(b)). This is because all matrix elements of the form $\langle \alpha_i | V | \beta_j \rangle$ vanish: $\langle \alpha_i | V | \beta_j \rangle = \frac{1}{2}(\langle \psi_i | + \langle \bar{\psi}_{i+1} |)(\xi |\bar{\psi}_{j+1}\rangle - \xi |\psi_j\rangle) = 0$.

As there are no energy corrections to R up to order $N-1$ in V , we can replace the perturbed energy E_N with the unperturbed energy $\epsilon_R = 0$.

The $N-1$ order wavefunction correction is thus given by:

$$\begin{aligned} |R^{(N-1)}\rangle &= |\alpha_1\rangle \frac{1}{0-1} \langle \alpha_1 | V | \alpha_2 \rangle \\ &\times \dots \times |\alpha_{N-1}\rangle \frac{1}{0-1} \langle \alpha_{N-1} | V | R \rangle \\ &+ |\beta_1\rangle \frac{1}{0+1} \langle \beta_1 | V | \beta_2 \rangle \\ &\times \dots \times |\beta_{N-1}\rangle \frac{1}{0+1} \langle \beta_{N-1} | V | R \rangle \end{aligned}$$

Other contributions to the wavefunction at this order do not reach the first lattice site and thus do not contribute to the edge-state effective Hamiltonian.

Now, $\langle \alpha_i | V | \alpha_{i+1} \rangle = \xi$ and $\langle \beta_i | V | \beta_{i+1} \rangle = -\xi$.

Thus we obtain the energy correction at order N as:

$$E_R^{(N)} = -2\xi^N$$

Reintroducing the factor of λ in 7, we obtain the N -th order effective Hamiltonian for the edge-states in the $\{|R\rangle, |L\rangle\}$ basis (on subtracting contributions to the identity) as:

$$V_{edge} = \lambda \begin{bmatrix} 0 & -2\xi^N \\ -2\xi^N & 0 \end{bmatrix} \quad (12)$$

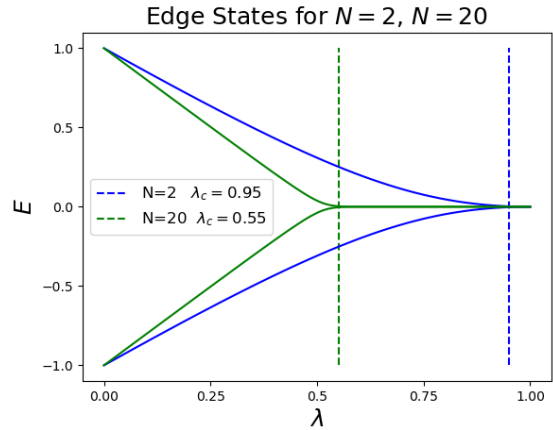


Figure 7: For a lattice with 2 sites, the degeneracy lifts on deviating even slightly from $\lambda = 1$: The topological protection is much weaker than for the lattice with 20 sites.

There is thus a gap of $\Delta = 4\lambda\xi^N$ between the edge-modes at the lowest nonvanishing order of perturbation theory. We note that the effective Hamiltonian and the result for the energy gap are only valid within the nontrivial phase and diverge in the trivial

phase as $N \rightarrow \infty$. This is as expected: the edge-modes no longer exist in the trivial phase, and the perturbation theory breaks down.

In the nontrivial phase, $\lambda > \frac{1}{2}$ and thus $\xi < 1$. The process required to break the degeneracy is suppressed exponentially. This explains why the edge-modes remain *gapless* throughout the nontrivial phase.

The suppression of this process in the nontrivial phase is dependent on the number of links on the lattice, and for a smaller lattice it is expected that the degeneracy breaks below a value of λ larger than $\lambda_c = \frac{1}{2}$. Numerically, on a two-site lattice, we find that the critical point shifts to $\lambda_c = 0.95$ (see Fig. 7), as compared to $\lambda_c = 0.55$ for a lattice with 20 sites.

Breaking the degeneracy of the edge-states requires a *global perturbation* along the entire length of the lattice. This is indicative of the fact that this degeneracy is *topologically protected* and hence robust against local perturbations.

VI. CONCLUSION

The explicit demonstration of time-reversal symmetry breaking and band inversion in section III provides a microscopic basis for the dimensional extension arguments for the topological phase transition

as discussed in [2].

The real-space analysis we have presented in sections IV and V makes use of the exactly-solvable limit within the nontrivial phase to obtain an exact expression for the edge-state wavefunctions. Deviations from this limit allow us to understand the topological phase transition in terms of the *delocalisation and ultimate disappearance* of these gapless edge-modes as the system passes from the nontrivial to the trivial phase. We note that only a *global transformation* can break the edge-mode degeneracy and change the topological class of the system. We also find that the extent of topological protection depends on the length of the system.

The real-space description of the model we have discussed does not rely on lattice-translation symmetry. This opens up the possibility of analysing the topological phase transition in disordered topological insulators using the effective edge-state Hamiltonian. Our analysis is significant in that it both illustrates the formation of edge-modes and their topological protection without any reference to the reciprocal space.

Declaration The Authors have no competing interests to declare.

Acknowledgements We would like to thank Ritwik Das and Pritam Sarkar for useful discussions and Sudeshna Dasgupta for valuable comments on the manuscript.

-
- [1] Vanderbilt - Berry phases in Electronic Structure Theory - ISBN 978-1-107-15765-1
 - [2] Asbóth, Oroszlány, Pályi - A Short Course on Topological Insulators. <https://arxiv.org/abs/1509.02295>
 - [3] Haldane - Model for a Quantum Hall Effect without Landau Levels: Condensed-Matter Realization of the "Parity Anomaly" - Phys. Rev. Lett. 61, 2015 - (Oct. 31 1988)
 - [4] Andrews, Reis, Harper, Roy - Localization renormalization and quantum Hall systems <https://arxiv.org/abs/2310.14074>
 - [5] Qi, Wu, Zhang - Topological quantization of the spin Hall effect in two-dimensional paramagnetic semiconductors - Phys. Rev. B 74, 085308 (10 Aug. 10 2006)
 - [6] Su, Schrieffer, Heeger - Solitons in Polyacetylene - Phys. Rev. Lett. Vol. 42, No. 25 (Jun. 18, 1979)
 - [7] Kohmoto - Topological Invariant and the Quantisation of Hall conductance - Annals of Physics Vol. 160, (Apr. 1, 1985)
 - [8] Kane - Topological Band Theory and the Z_2 Invariant - Contemporary Concepts of Condensed Matter Science, Elsevier 2013.
 - [9] Qi, Hughes, Zhang - Topological Field Theory of Time-Reversal Invariant Insulators <https://arxiv.org/abs/0802.3537>
 - [10] Baym - Lectures On Quantum Mechanics - ISBN 13: 978-0-8053-0667-5
- Note: All figures, except graphs, have been have been created using the tikz package. <https://tikz.dev/>